WORK AT THE SPEED OF THOUGHT

Take clinical efficiency to new levels through smart, personalized automation.

RayStation

RayCare

ADVANCING CANCER TREATMENT

RaySearch Laboratories

Technical Note

PMP

Progress in Medical Physics 33(4), December 2022
https://doi.org/10.14316/pmp.2022.33.4.164
eISSN 2508-4453

50–300 kVp X-ray Transmission Ratios for Lead, Steel and Concrete

Tae Hwan Kim[2,5], Kum Bae Kim[3], Geun Beom Kim[1], Dong Wook Kim[3], Sang Rok Kim[2], Sang Hyoun Choi[1]

[1]Research Team of Medical Physics, Korea Institute of Radiological & Medical Sciences, [2]Radiation Safety Section, Korea Institute of Radiological & Medical Sciences, [3]Department of Radiation Oncology, Korea Institute of Radiological & Medical Sciences, [4]Department of Radiation Oncology, Yonsei Cancer Center, Yonsei University College of Medicine, Seoul, [5]Department of Medical Physics, Korea University, Sejong, Korea

Received 8 December 2022
Revised 23 December 2022
Accepted 23 December 2022

Corresponding author
Sang Hyoun Choi
(sh524mc@gmail.com)
Tel: 82-2-970-1590
Fax: 82-2-970-1962

Corresponding author
Sang Rok Kim
(kim@kirams.re.kr)
Tel: 82-2-970-1346
Fax: 82-2-970-1963

The number of facilities using radiation generators increases and related regulations are strengthened, the establishment of a shielding management and evaluation technology has become important. The characteristics of the radiation generator used in previous report differ from those of currently available high-frequency radiation generators. This study aimed to manufacture lead, iron, and concrete shielding materials for the re-verification of half-value layers, tenth-value layers, and attenuation curve. For a comparison of attenuation ratio, iron, lead, and concrete shields were manufactured in this study. The initial dose was measured without shielding materials, and doses measured under different types and thicknesses of shielding material were compared with the initial dose to calculate the transmission rate on 50–300 kVp X-ray. All the three shielding materials showed a tendency to require greater shielding thickness for higher energy. The attenuation graph showed an exponential shape as the thickness decreased and a straight line as the thickness increased. The difference between the measurement results and the previous study, except in extrapolated parts, may be due to the differences in the radiation generation characteristics between the generators used in the two studies. The attenuated graph measured in this study better reflects the characteristics of current radiation generators, which would be more effective for shield designing.

Keywords: Half-value layers, Tenth-value layers, Attenuation rate, Radiation protection, X-ray attenuation

Introduction

In the "Enforcement Decree of the Serious Accidents Punishment Act," which took effect on January 27, 2022, acute radiation syndrome (ARS) caused by exposure to ionizing radiation is one of several occupational diseases. ARS owing to ionizing radiation in three or more people in a year, is defined as a "serious industrial accident." Regulations have been strengthened for the safe use of industrial radiation generators and the minimization/optimization of radiation exposure dose in radiation workers and people who frequently access related radiation-generating facilities [1]. In 2018, 6,372 institutions in Korea used industrial radiation generators. The number of institutions using industrial radiation generators increased by 5.1% to 6,696 in 2019 and 3% to 6,898 in 2020 compared with those in previous years, showing a mean annual increase of 4% [2]. As the number of facilities using radiation generators increases

Copyright © 2022 Korean Society of Medical Physics
This is an Open-Access article distributed under the terms of the Creative Commons Attribution Non-Commercial License (http://creativecommons.org/licenses/by-nc/4.0) which permits unrestricted non-commercial use, distribution, and reproduction in any medium, provided the original work is properly cited.

and related regulations are strengthened, the establishment of a shielding management and evaluation technology that can prevent human accidents caused by excessive exposure to radiation in workers and frequent visitors has increasingly become important.

To evaluate the shielding safety of facilities that use radiation generators, permeability coefficients for primary, scattered, and leakage radiations are calculated, and the type and thickness of the shielding material are determined based on the half-value layer (HVL), tenth-value layer (TVL), and attenuation curve data according to the energy level and shielding material suggested in NCRP Report No. 49 [3]. However, NCRP Reports No. 49 and 51, which are commonly used as a reference for the evaluation of shielding safety and design, were published in 1976 and 1977, respectively [4]. Although the radiation generators in these reports are different from currently available generators, the two reports are still used as reference data for evaluating the safety of facilities that use industrial radiation generators. In 1972, Trout and Kelley [5] used a single-phase, full-wave radiation generator to measure the attenuation ratio of broad-beam X-rays in the range of 50 to 300 kVp in lead. The characteristics of the radiation generator used in that study differ from those of currently available high-frequency radiation generators [6]. Additionally, several studies evaluated and compared the characteristics of critical factors of radiation generators with previous reports (NCRP Report No. 49), showing that the characteristics of the radiation generators were different [5,7,8]. Therefore, these differences in radiation generators and radiation quality may limit the use of data in NCRP Report No. 49 for designing accurate shielding. The primary, scattered, and leakage radiations presented in NCRP Report No. 49 must be re-evaluated to optimize the safety of current industrial radiation generators [9]. Thus, this study aimed to manufacture lead, iron, and concrete shielding materials for the re-verification of HVL,

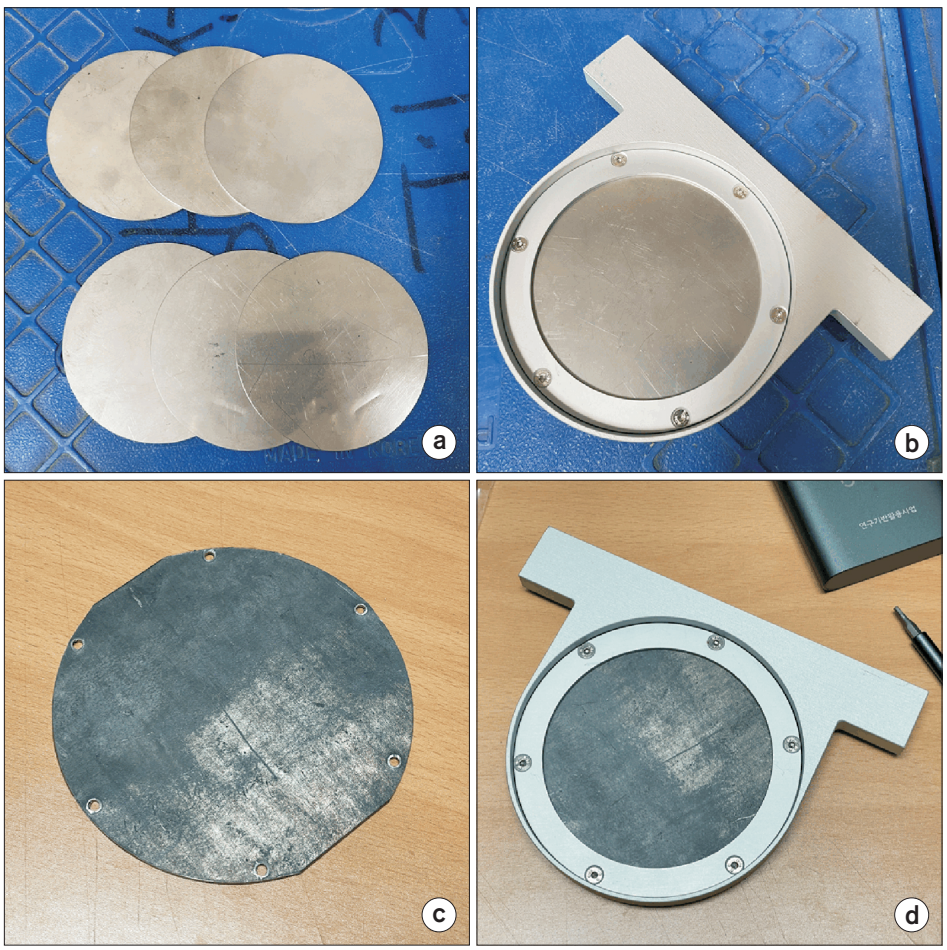

Fig. 1. The lead shielder and steel shielder. A steel and lead plate was cut (a, c) and assembled with frame (b, d).

TVL, and attenuation curve for the energy level and shielding material suggested in NCRP Report No. 49. Herein, the attenuation rate in each shielding material by energy level was evaluated and compared with the values suggested in NCRP Report No. 49.

Materials and Methods

1. Manufacturing of shields

The shielding materials suggested in NCRP Report No. 49 are iron, lead, and concrete. For a comparison of attenuation ratio, iron, lead, and concrete shields were manufactured in this study. The lead shields were manufactured with three different thicknesses of 0.2, 0.5, and 1.0 mm. The iron shields were manufactured with the four different thicknesses of 0.5, 1.0, 2.0, and 5.0 mm, and the concrete shields were manufactured with the six different thicknesses of 3, 5, 7.5, 10, 20, and 50 mm. An attenuation graph including the HVL and TVL was obtained. The shields were manufactured according to the tray standard on the front of the radiation generator for installation. The lead and iron shields were processed as shown in Fig. 1a, c and manufactured to satisfy the tray specification in Fig. 1b, d.

As concrete has low ductility, concrete shields cannot be manufactured using the same processes as lead and iron shields [10]. As shown in Fig. 2, a mold identical to the specification of the frame was produced with a 3D printer and filled with concrete. The thickness of the manufactured shields was evaluated using a calibrated caliper. The thickness and configurable range of thickness of each shielding material are shown in Table 1.

2. Attenuation ratio graph measurement

The attenuation ratio of radiation for different thicknesses

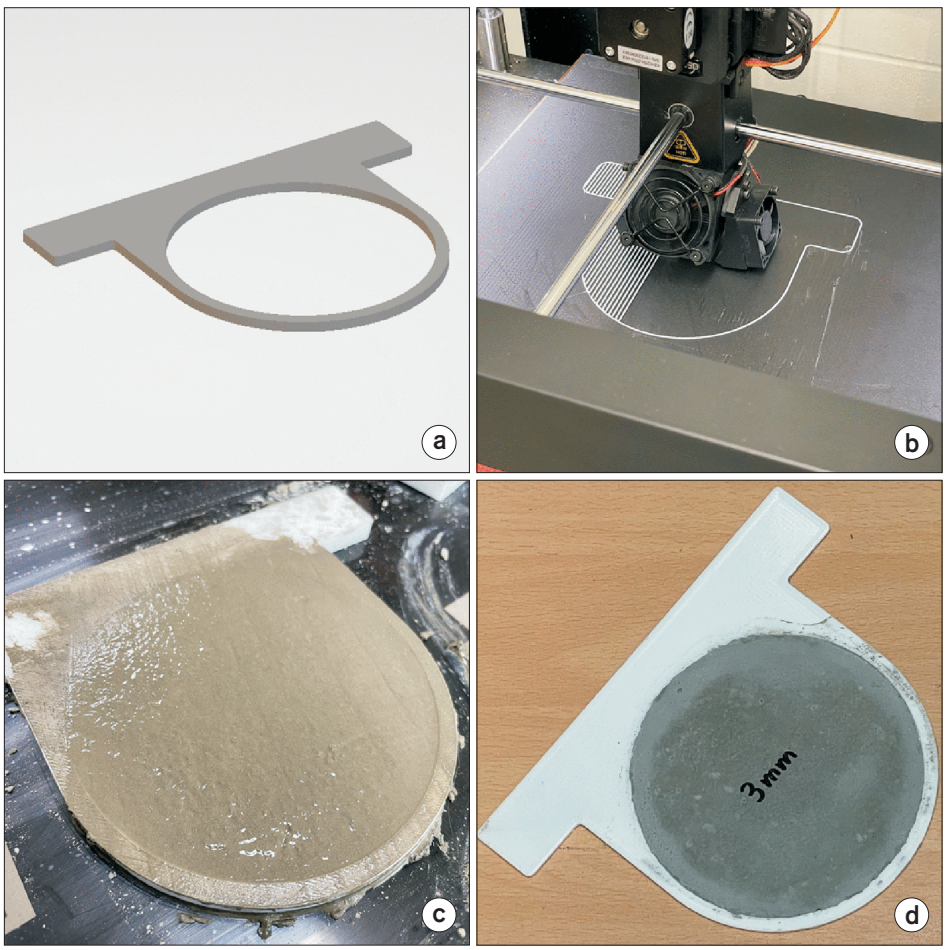

Fig. 2. Making process of the concrete shielder. To work with 3D printer, the concrete shielder was designed like (a). Then the mold (b) was made and was filled with concrete (c). The Concrete needs some days for hardening (d).

of shields was measured at the X-ray irradiation facility in the Medical Radiation Quality Control Center of Korean Association for Radiation Application. An MXR-320/26 (Comet AG, Wünnewil-Flamatt, Switzerland) radiation generator with a maximum tube voltage of 320 kV and a maximum tube current of 26 mA was used [11]. The shielded radiation dose was measured with Exradin A3 Spherical Ion Chamber, 3.6 cc (Standard Imaging, Middleton, WI, USA), an ion chamber commonly used to measure standard X-rays. The results were cross-validated by measuring with RaySafe 452 survey meter (FLUKE Biomedical, Everett, WA, USA), a GM+solid-state sensor type detector, under the same conditions. To correct for temperature and air pressure in the irradiation facility, the temperature and air pressure were measured simultaneously with radiation dose, using the multi-functional precision thermometer CTR3000 (WIKA, Klingenberg am Main, Germany) and precision pressure indicator CPG2500 (WIKA), respectively [12-14]. The experimental devices were configured as shown in Fig. 3a to reflect the layout used in the measurement of dose and half-layer in "AAPM Protocol TG-61" in Fig. 3b [15,16].

Table 1. Thickness and quantity of each shielding material

Shielding material	Thickness (mm)	Configurable thickness range (T)
Lead	0.2 0.5 1.0	0.2 mm≤T≤5.1 mm
Steel	0.5 1.0 2.0 5.0	0.5 mm≤T≤22 mm
Concrete	3.0 5.0 7.5 10.0 20.0 50.0	3.0 mm≤T≤117 mm

The same conditions used in NCRP Report No. 49 were used to compare our results with previous findings. The initial dose was measured without shielding materials, and doses measured under different types and thicknesses of shielding material were compared with the initial dose to calculate the transmission rate. Measurements were made within the range of possible configurations of the manufactured shields by reflecting the additional filter conditions for each energy level and type of shielding material (Table 2). Unlike lead and concrete, additional filter information is not specified for iron in NCRP Report No. 49. Thus, in this study, additional filter conditions for each energy level for lead were used for iron. The density of the manufactured concrete shields was 2.01 g/cm^3, and the density of the concrete shields used in NCRP Report No. 49 was 2.35 g/cm^3 [3,17]. The difference in the density of concrete shields was corrected in the attenuation ratio curve of this study. Under the different conditions, X-rays were irradiated for 70 seconds. The average and standard deviation were calculated for the charge measured in the ion chamber at one-second interval during irradiation.

Results and Discussion

To cross-validate the ion chamber used in the study, the

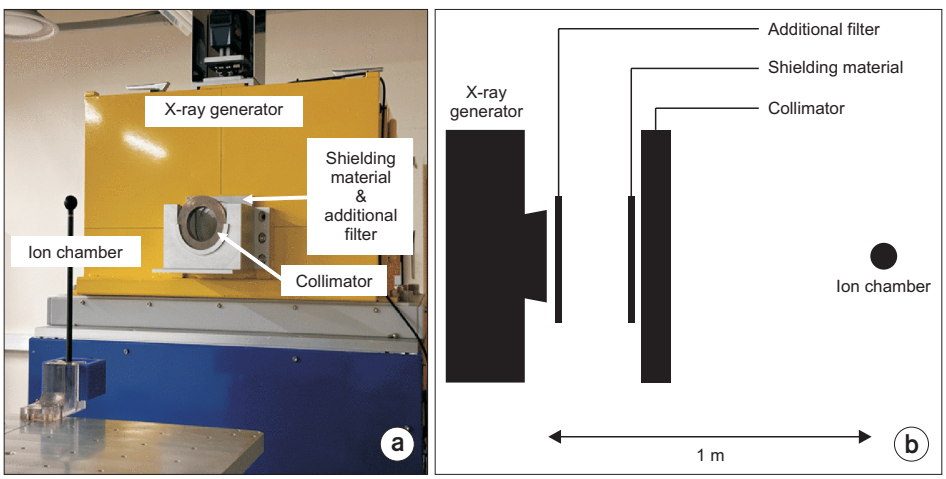

Fig. 3. Arrangement of performed experiments component (a), AAPM protocol TG-61 arrangement (b).

attenuation ratios according to the thickness of the lead shields measured using the A3 ion chamber and RaySafe 452 survey meter were compared. The results are shown in Fig. 4. Table 3 shows the measured HVL and TVL. Compared with the values suggested in NCRP Report No. 49, the two ion chambers showed a difference of 0.34% for HVL and 1.93% for TVL. In detail, compared with the values suggested in NCRP Report No. 49, at 150 kVp, the RaySafe 452 survey meter showed a difference of 1.68% for HVL and 0.30% for TVL in the case of lead, and the A3 ion chamber showed a difference of 1.34% for HVL and 1.63% for TVL in the case of lead.

Table 2. Experimental condition

Shielding material	X-ray tube potential energy (kVp)	Additional filter (mmAl)
Lead, steel	50	0.5
	70	1.5
	100	2.5
	125	2.5
	150	3.0
	200	3.0
	250	3.0
	300	3.0
Concrete	50	1.0
	70	1.5
	100	2.0
	125	3.0
	150	3.0
	200	3.0
	250	3.0
	300	3.0

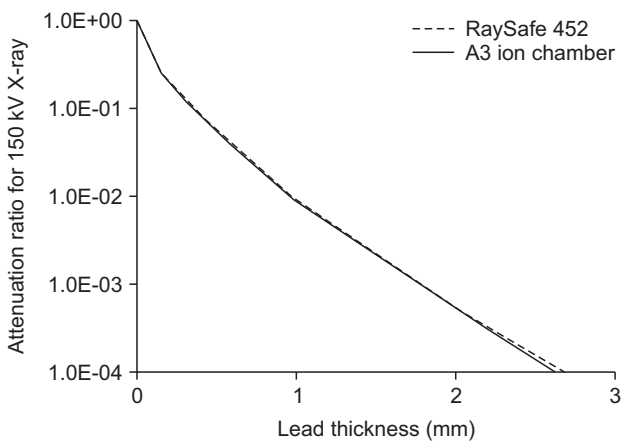

Fig. 4. Attenuation ratio curve compared with RaySafe 452 and A3 Ion chamber.

Fig. 5 shows the measured attenuation ratio of each shielding material. In the attenuation ratio curve, values that exceeded the detectable range or shielding configuration range of the A3 ion chamber were extrapolated through linear interpolation. All the three shielding materials showed a tendency to require greater shielding thickness for higher energy. The attenuation graph showed an exponential shape as the thickness decreased and a straight line as the thickness increased.

The attenuation graph for different thicknesses of each shielding material measured under the proposed energy conditions was different from the graph shown in NCRP Report No. 49. Compared with the graph shown in NCRP Report No. 49, the attenuation graph for lead showed lower shielding of radiation as the shielding thickness decreased and more excellent shielding of radiation as the shielding thickness increased (Fig. 6). As the shielding thickness increased, the coefficient of variation of the measured value increased. Subsequent extrapolation based on these values with a significant coefficient of variation may be attributed to this result. Therefore, in future studies, an ion chamber with a greater detection range would need to be used.

Compared with the graph presented in NCRP Report No. 49, the measured attenuation ratio curve for concrete in this study showed greater radiation shielding (Fig. 7). The limitations in the density of the produced concrete shielding were corrected in the attenuation ratio curve; however, the precise density was not reflected. Therefore, in future studies, concrete shielding with identical density needs to be manufactured for re-evaluation.

Table 3. Measured HVL/TVL of lead compared with RaySafe 452 and A3 Ion chamber

Reference	For 150 kV X-ray	
	HVL (mm)	TVL (mm)
NCRP Report No. 49	0.3	0.99
Detector		
RaySafe-452	0.295 (1.68%)	0.993 (0.30%)
A3 Ionchamber	0.296 (1.34%)	0.974 (1.63%)

HVL, half-value layer; TVL, tenth-value layer.
Difference with NCRP Report No.49 and measured value is described in parentheses.

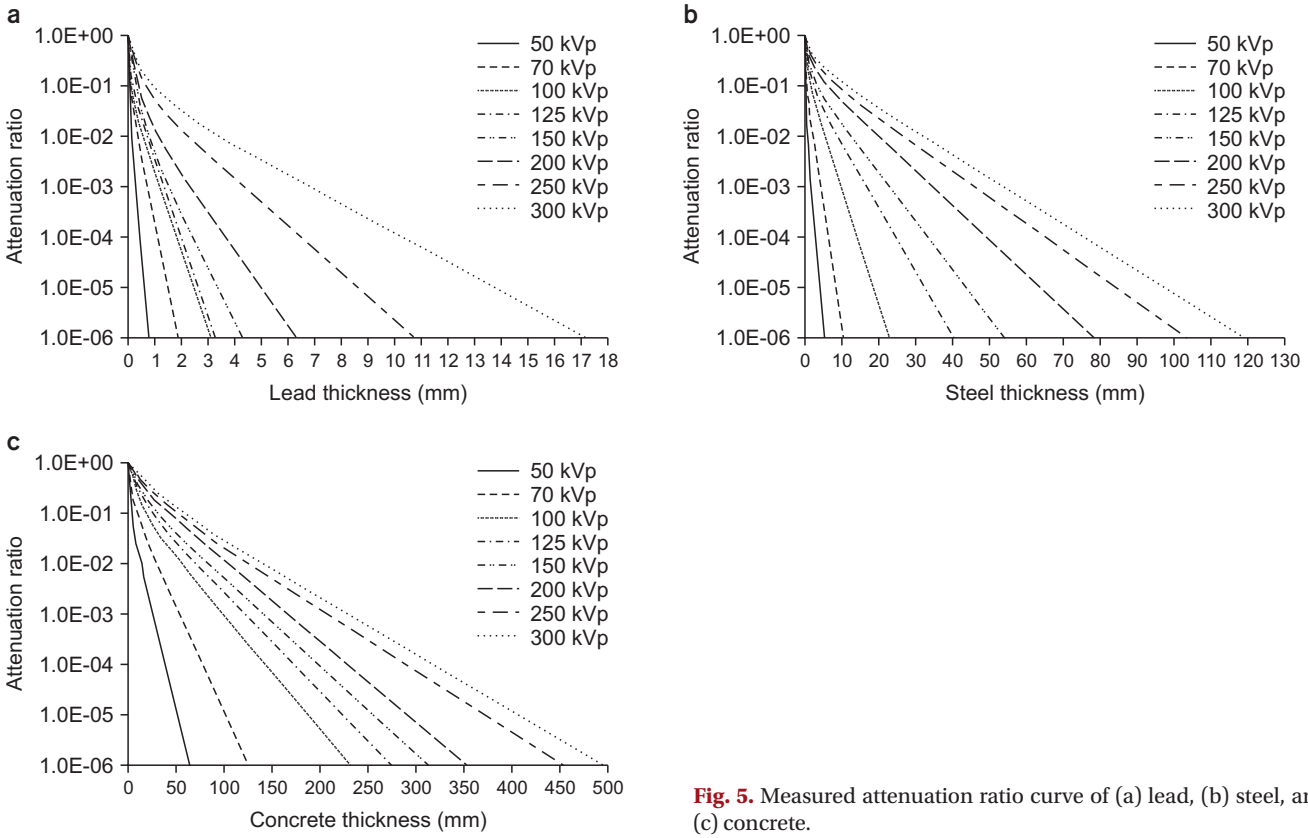

Fig. 5. Measured attenuation ratio curve of (a) lead, (b) steel, and (c) concrete.

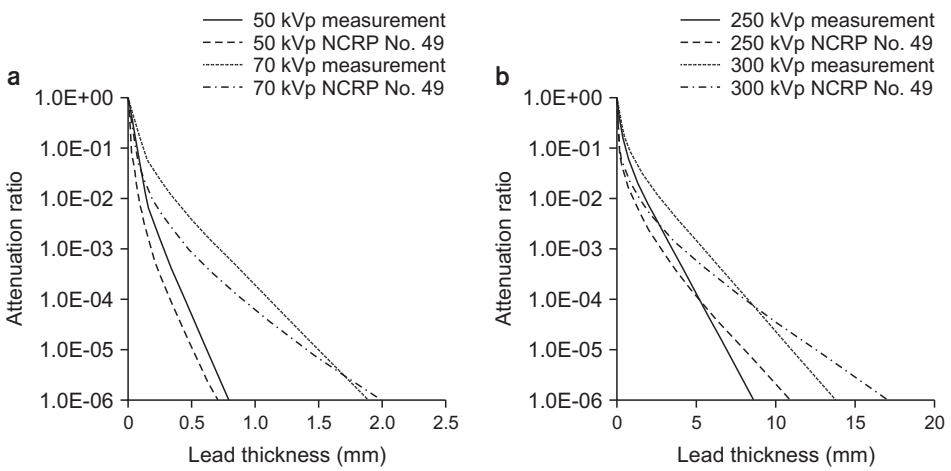

Fig. 6. Attenuation ratio curve for lead compared with measurements and NCRP Report No. 49, 50 kVp/70 kVp (a), 250 kVp/300 kVp (b).

Conclusions

This study verified the validity of critical factors in the assessment of shielding safety in NCRP Report No. 49. Lead, iron, and concrete shields were manufactured to measure attenuation ratios, HVL, and TVL. To verify the validity, the measured attenuation graph was compared with that in NCRP Report No. 49. Differences were observed between the two attenuation graphs. The difference between the two graphs, except in extrapolated parts, may be due to the differences in the radiation generation characteristics between the generators used in the two studies. The attenuated graph measured in this study better reflects the characteristics of current radiation generators, which would be more effective for shield designing. However, further studies must be conducted for the extrapolated data of the measured

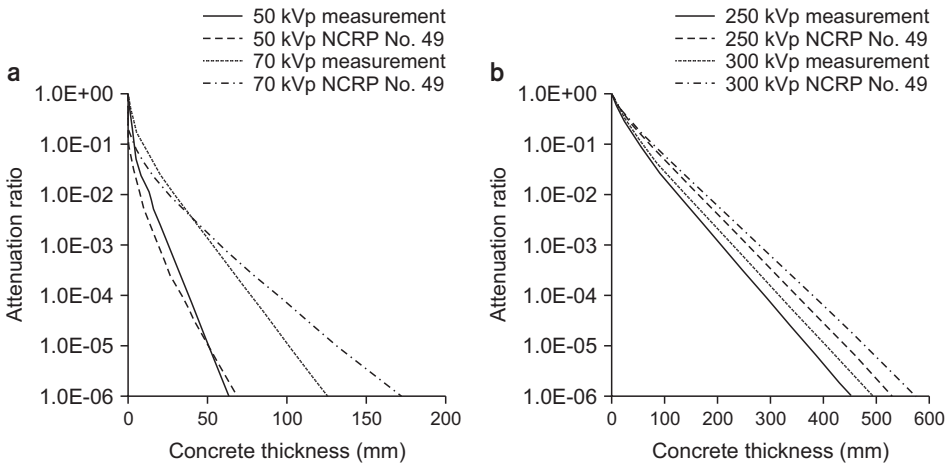

Fig. 7. Attenuation ratio curve for concrete compared with measurements and NCRP Report No. 49 50 kVp/70 kVp (a), 250 kVp/300 kVp (b).

attenuation graph. Therefore, a follow-up study will be performed using a detector with a broader range of detection and shields that are adequate for the conditions of concrete shields suggested in NCRP Report No. 49.

Acknowledgments

This research was supported by the Nuclear Safety Research Program through the Korea Foundation of Nuclear Safety (KoFONS) using the financial resource granted by the Nuclear Safety and Security Commission (NSSC) of the Republic of Korea (No.2003013 & 2205013).

Conflicts of Interest

The authors have nothing to disclose.

Availability of Data and Materials

The data that support the findings of this study are available on request from the corresponding author.

Author Contributions

Conceptualization: Tae Hwan Kim, Kum Bae Kim, Geun Beom Kim, Dong Wook Kim, Sang Rok Kim, and Sang Hyoun Choi. Data curation: Tae Hwan Kim, Sang Hyoun Choi, and Sang Rok Kim. Formal analysis: Tae Hwan Kim, Sang Hyoun Choi, and Sang Rok Kim. Funding acquisition: Sang Hyoun Choi. Investigation: Tae Hwan Kim, Sang Rok Kim, and Sang Hyoun Choi. Methodology: Dong Wook Kim, Sang Rok Kim, and Sang Hyoun Choi. Project administration: Sang Hyoun Choi. Resources: Sang Hyoun Choi. Software: None. Supervision: Sang Hyoun Choi. Validation: Sang Rok Kim and Sang Hyoun Choi. Visualization: Tae Hwan Kim. Writing – original draft: Tae Hwan Kim. Writing – review & editing: Sang Rok Kim and Sang Hyoun Choi.

References

1. Ministry of Science and ICT. Survey on the status of radiation/RI utilization. General table of usage of radioactive isotopes and radiation generators. Sejong: Ministry of Science and ICT, 2020 [cited 2022 Nov 29]. Available from: https://kosis.kr/statHtml/statHtml.do?orgId=127&tblId=TX_10504_A000
2. Korean Law Information Center. Enforcement decree of the serious accidents punishment act. Sejong: Korean Law Information Center, 2022 [cited 2022 Nov 29]. Available from: https://www.law.go.kr/eng/engLsSc.do?menuId=2&query=ENFORCEMENT%20DECREE%20OF%20THE%20SERIOUS%20ACCIDENTS%20PUNISHMENT%20ACT#liBgcolor0
3. National Council on Radiation Protection and Measurements (NCRP). Structural shielding design and evaluation for medical use of X rays and gamma rays of energies up to 10 MeV. Bethesda: NCRP. 1976; 49.
4. National Council on Radiation Protection and Measurements (NCRP). Radiation protection design guidelines for 0.1 to 100 MeV particle accelerator facilities. Washington,

D.C.: NCRP. 1977; 51.
5. Trout ED, Kelley JP. Scattered radiation from a tissue-equivalent phantom for x rays from 50 to 300 kVp. Radiology. 1972;104:161-169.
6. Kim TG, Cheon MW, Park YP. Comparison of output and radiation quality of X-rays according to the full-wave rectification method and dual-voltage rectification method of an X-ray generator. KIEEME. 2010;23:534-538.
7. Trout ED, Kelley JP, Lucas AC. Broad beam attenuation in concrete for 50 to 300-Kvp x-rays and in lead for 300 Kvp x-rays. Radiology. 1959;72:62-67.
8. Miller W, Kennedy RJ. X-ray attenuation in lead, aluminum, and concrete in the range 275 to 525 kilovolts. Radiology. 1955;65:920-925.
9. International Commission on Radiological Protection (ICRP). The 2007 Recommendations of the International Commission on Radiological Protection. ICRP. 2007; 103.
10. Gabriel T: The rise and fall of the thin concrete shell. Proceedings of the Second International Conference on Flexible Formwork. Bath: University of Bath; 2012:324-333.
11. Jang HG, Min JH, Han GT, Lee BH, Oh SJ. Establishment of the infrastructure for the quality assurance and the dissemination of radiation measurement standard in medicine. Sejong: Ministry of Science and ICT. 2019; 2014M2B8A3032609.
12. Cember H, Johnson TE. Introduction to health physics. New York: McGraw-Hill; 2009.
13. Torres Del Río J, Forastero C, Tornero-López AM, López JJ, Guirado D, Perez-Calatayud J, et al. Air density dependence of the soft X-ray PTW 34013 ionization chamber. Phys Med. 2018;46:109-113.
14. Lee CL, Kim HJ, Jeon SS, Cho HM, Nam S, Jung JY, et al. Comparison of radiation dose in the measurement of MDCT radiation dose according to correction of temperatures and pressure, and calibration of ionization chamber. Korean J Med Phys. 2008;19:49-55.
15. American Association of Physicists in Medicine (AAPM). AAPM protocol for 40–300 kV x-ray beam dosimetry in radiotherapy and radiobiology. Alexandria: AAPM. 2001; 76.
16. Kim JH, An SH, Oh YJ, Ji YS, Huh JY, Kang CM, et al. HVL Measurement of the miniature X-ray tube using diode detector. Korean J Med Phys. 2012;23:279-284.
17. Amin MN, Ahmad I, Iqbal M, Abbas A, Khan K, Faraz MI, et al. Computational AI models for investigating the radiation shielding potential of high-density concrete. Materials (Basel). 2022;15:4573.